Effect of Solute-Solute Correlations on Rapid Reactions in Supercritical Fluids

Shankar Ganapathy and James A. O'Brien
Dept. of Chemical Engineering, Yale University, New Haven, CT 06520

Theodore W. Randolph
Dept. of Chemical Engineering, University of Colorado, Boulder, CO 80309

Brownian and molecular dynamics simulations are used to study rapid bimolecular reactions at near-infinite dilution in near-critical and supercritical fluids. We probe the dynamics of both nonreactive and reactive collisions and measure rate constants for reaction and collision. Collision rate constants are nearly independent of bulk solvent density, but affected by local solute-solute density enhancements at a given density: their magnitudes depend on the length scale for molecular encounters (cybotactic radius) in the reaction through the equilibrium solute-solute radial distribution function. In contrast, reaction rate constants asymptotically approach the gas-kinetic limit at low densities and the Smoluchowski liquid-like limit at high densities. They also display the same radial dependence as collision rate constants at lower densities and a direct dependence on the cybotactic radius at higher densities (as in the Smoluchowski theory). Their behavior is explained in terms of a transition from a collision-limited regime at low densities to a diffusion-limited regime at higher densities. The transition between these regimes depends on the cybotactic radius and the density of the system, the interplay of which causes shifts in the transition region which depend not only on the properties of the near-critical solvent: they differ for different reactions, even at the same solvent density. This explains some of the apparent inconsistencies among previous experimental and computational studies of reactions in supercritical fluid media.

Introduction

There are certain classes of extremely rapid reactions where mass transfer is the rate-limiting step. Almost all free-radical reactions require so little activation energy that they are diffusion-controlled at liquid-like densities; examples of such reactions include atom recombinations, low molecular-weight free-radical reactions, and macroradical reactions such as free-radical polymerization (North, 1964). While these limitations could be relieved by carrying out these reactions in the gas phase, gas-phase reactant solubilities are often extremely low. The supercritical fluid phase provides a balance between the high solubilities provided by liquids and the high mass-transfer rate achievable in gases.

The use of supercritical fluids (SCFs) as reaction media is an area of current technological development. Some of the unique features that characterize SCFs are liquid-like densities, gas-like viscosities, and diffusivities that are intermediate between typical gas and liquid values. Perhaps the most important feature is the ability to vary widely these properties of a SCF using small changes in temperature and pressure. Despite these potential advantages, fundamental understanding of the effect of supercritical fluid structure on reactivity is still incomplete.

Reactivity of a solute in a supercritical solvent is strongly dependent on its local environment (Johnston and Haynes, 1987). Studies of reactions in supercritical fluid media have shown that local solvent structure has a substantial effect on reaction rate constants, which has been explained in terms of local density variations of the solvent in the environment sur-

Correspondence concerning this article should be addressed to J. A. O'Brien.

rounding the solute (Johnston and Haynes, 1987). Local density augmentation of solvents around solute molecules has been measured in various spectroscopic studies (Kim and Johnston, 1987; Kajimito et al., 1988; Yonker and Smith, 1988; Johnston et al., 1989; Brennecke and Eckert, 1988, 1989; Brennecke et al., 1990; Betts et al., 1992; Carlier and Randolph, 1993). Computational approaches and integral equation theories have provided further evidence of these local density variations. Molecular dynamics (MD) simulations of Knutson et al. (1992) showed local density enhancements of supercritical carbon dioxide around dilute naphthalene solutes which qualitatively resemble enhancements measured using fluorescence spectroscopy. Debenedetti (1987) has applied fluctuation theory analysis to partial molar volume data for naphthalene in supercritical carbon dioxide, and has predicted an excess of over 100 solvent molecules around each solute molecule. Such solvent excesses have also been calculated using integral equation theory, using the Percus-Yevick closure for a model of xenon at infinite dilution in neon (Wu et al., 1989).

Experimental studies of reaction rate constants have not clearly shown how local density enhancements (either solvent about solute, or solute about solute) affect reactions in general. Johnston and Haynes (1987) studied the unimolecular decomposition of α-chlorobenzylmethyl ether and found that solvent-solute clustering increases the reaction rate. Chateauneuf et al. (1992) reported that the rate of ketyl radical formation from excited state benzophenone is enhanced by the clustering of 2-propanol which is a cosolvent. In addition, electron paramagnetic resonance spectroscopy (EPR) spectroscopic studies of the Heisenberg spin-exchange reaction between di-*tert*-butyl nitroxide radicals in supercritical ethane provided evidence that local density enhancements of solvents around solutes affects reaction rate constants. There was no evidence, however, of any effect of solute-solute clustering on the reaction rate (Randolph and Carlier, 1992). Similarly, steady-state and time-resolved fluorescence spectroscopic studies of the photophysics of pyrene emission in supercritical CF_3H indicated that solvent-solute clustering strongly affects the pyrene excimer reaction, but that solute-solute clustering has no effect (Zagrobelny and Bright, 1992). However, laser flash photolysis studies of the triplet-triplet annihilation process of benzophenone and the self-termination reaction of benzyl radical in supercritical carbon dioxide and ethane showed no effect of either the solvent-solute or solute-solute clustering on the reaction rate constants (Roberts et al., 1993). Studies of the photolysis of iodine (Otto et al., 1984) showed solvent-solute clustering to have a strong effect on the reaction rate (Combes et al., 1992) and studies of the photodimerization of 2-cyclohexen-1-one indicated that solute-solute clustering affects the rate of cyclohexenone dimerization (Combes et al., 1992).

There have been several experimental and theoretical studies on the transition behavior of the reaction rate constants for recombination, dissociation, and isomerization reactions over a wide density range from low density gas-phase conditions to compressed liquids (Kramers, 1940; Troe, 1986; Zawadzki and Hynes, 1989; Schroeder and Troe, 1987). These studies dealt with various aspects that characterize this class of reactions such as intramolecular rearrangements, intermolecular energy transfer, radiationless electronic transitions, diffusive fragment separation, and reactant approach. This article deals with a simplified system whose reactivity is not a function of the above factors, recognizing that our predictions cannot capture all of the complexities represented in these reactions.

The local microstructure around reacting solutes in supercritical media is not just spatial, but also temporal. For example, O'Brien and co-workers (1993) carried out molecular dynamics and Monte-Carlo simulations mimicking very dilute solutions of di-*tert*-butyl nitroxide (DTBN) radicals in supercritical ethane, and showed that long-lived solvent clusters form around the solutes at densities somewhat below the critical density. Corti and Debenedetti (1993) recently reported the existence of similarly long-lived solvent-solute clusters in the pyrene-carbon dioxide system. To investigate directly the effects of the local microstructure (both solvent-solute and solute-solute) on the reaction rate constants, we have carried out Brownian dynamics and molecular dynamics simulation studies. Our simulations are designed to mimic the fast bimolecular Heisenberg spin-exchange reaction, which is diffusion-limited in most liquid solvents. Theoretical and computational evidence of large solvent-solute and solute-solute clustering have not been unequivocally corroborated by experimentally measured reaction rates; this discrepancy motivates our microscopic level studies through computer simulation of reactions.

Background and Methodology

Equilibrium Brownian dynamics (BD) and molecular dynamics (MD) simulations were carried out to model the Heisenberg spin-exchange reaction of DTBN in near-critical and supercritical ethane. Details of the Heisenberg spin-exchange reaction are provided in some detail elsewhere (Carlier and Randolph, 1993). Spin exchange is an extremely fast bimolecular reaction in which the collision of radicals with opposite spin states results in an exchange of spin states. Because they differ only in spin states, the products of the reaction are chemically identical to the reactants. In our computations, ethane and DTBN were approximated as Lennard-Jones (L-J) molecules having the intermolecular potential:

$$\Gamma(r) = \begin{cases} 4\epsilon\left[\left(\frac{\sigma}{r}\right)^{12} - \left(\frac{\sigma}{r}\right)^{6}\right] & r < r_c \\ 0 & r \geq r_c \end{cases} \tag{1}$$

All quantities were made dimensionless using the L-J parameters in the following fashion (Allen and Tildesley, 1987):

$$T^* \equiv \frac{kT}{\epsilon} \qquad \text{temperature}$$

$$\rho^* \equiv \rho\sigma^3 \qquad \text{density}$$

$$\Delta t^* \equiv \frac{\Delta t}{(\sigma\sqrt{m/\epsilon})} \qquad \text{timestep}$$

$$r^* \equiv \frac{r}{\sigma} \qquad \text{length}$$

$$D^* \equiv D\frac{\sqrt{m/\epsilon}}{\sigma} \qquad \text{diffusivity}$$

Table 1. Lennard-Jones Parameters Used in the Simulations

	σ_{ij} [Å]	ϵ_{ij} [kcal/mol]
Ethane-Ethane	5.22	0.386
Ethane-DTBN	6.89	0.578
DTBN-DTBN	9.09	0.865

For the purposes of making clearer their relationship to the critical point, some results are expressed in *reduced* form instead, that is, normalized with respect to the corresponding critical quantity as follows:

$$T_r \equiv T/T_c = T^*/T_c^* \quad \text{temperature}$$

$$\rho_r \equiv \rho/\rho_c = \rho^*/\rho_c^* \quad \text{density}$$

The critical properties used to form the ratios are those of the L-J fluid, which have been computed precisely by Smit (1989) to be $\rho_{c,LJ}^* = 0.31$ and $T_{c,LJ}^* = 1.31$.

For the MD simulations, the solvent L-J parameters were used as the nondimensionalizing parameters, while for the BD calculations, the solute L-J parameters were used. A cutoff radius (see Eq. 1) of $r_c = 3.0\,\sigma_{22}$ was used in the BD calculations, and for the MD simulations, $r_c = 3.6\,\sigma_{11}$ was used. The L-J parameters for ethane are from Prausnitz (1969). The technique used to estimate the L-J parameters for DTBN is described by O'Brien et al. (1993). Table 1 lists the L-J parameters that were used in the simulations (ethane = 1, DTBN = 2).

Brownian dynamics simulations

The basis of Brownian dynamics is the approximation of the solvent as a structureless viscous medium, as opposed to discrete molecules. We have used the BD method to probe the interactions between solute (DTBN) molecules in a solvent-effective viscosity field (which represents ethane). The solute molecules do not interact with the individual molecules of the medium; instead the medium (which behaves like a continuum) exerts a stochastic force on the solutes. Consequently, no explicit solute-solvent and solvent-solvent interactions are considered.

BD simulations were carried out by numerically integrating the Langevin equation using the "velocity-first" scheme (Ermak and Buckholtz, 1980). The BD technique is based on the Langevin equation of motion of a particle, which is integrated numerically to solve for the trajectories of the solute molecules. The Langevin equation is:

$$m\frac{dv}{dt} = -m\beta v + F + X \qquad (2)$$

where $\beta = kT/mD_{12}$ for equilibrium Brownian motion. The first term in the Langevin equation, $-m\beta v$, is the frictional or drag term. This drag force is assumed to be Stokesian in nature, but a suitable slip correction factor can be added if necessary. The term F is the external (in this case intermolecular) force, while X is the Brownian force which represents the constant buffeting of the solute molecules by the molecules of the fluid medium. It is assumed that this Brownian force is independent of v, the velocity, and it is also assumed to vary rapidly compared to variations in the velocity (Chandrasekhar, 1943).

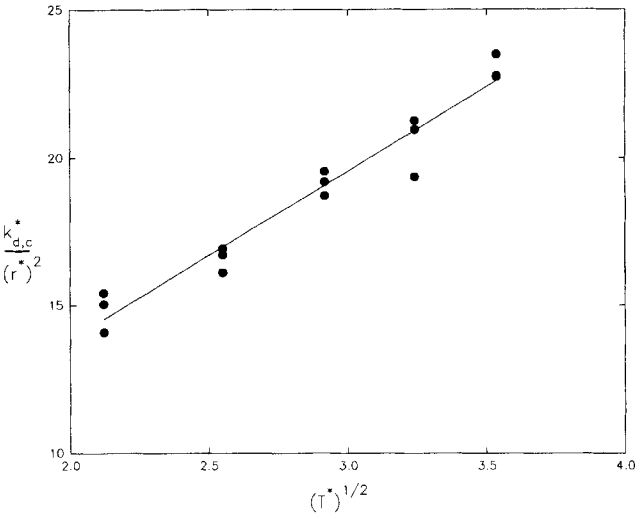

Figure 1. Collision rate constant, $k^*_{d,c}$ vs. the square root of temperature, $\sqrt{T^*}$.

$k^*_{d,c}$s are normalized by the square of the dimensionless collision radius. These measurements were carried out at three different collision radii; temperature is in solute L-J units. The variation is linear, as predicted from kinetic theory.

The integration scheme used assumes that the forces are essentially constant over a timestep which must, therefore, be chosen carefully. The timestep chosen for our particular simulation was based on the two-fold requirements that the forces should not change more than 5% over a given timestep, and the maximum displacements of the molecules should be comparable to a single diffusive step. All of the production BD simulations used a constant timestep of $\Delta t^* = 0.0064$ in solute L-J units. Simulation runs as long as 600,000 steps were carried out, especially for the reactive collision dynamics. The effective density of the system was changed by changing the value of the input diffusion coefficient; this was precomputed in a MD simulation. The Verlet neighbor list technique (Allen and Tildesley, 1987) modified with an automatic list updating scheme (Chialvo and Debenedetti, 1990, 1991) was implemented to speed up the simulations.

A useful check of our simulations is given by kinetic theory, which predicts that the collision rate constant is directly proportional to the square root of the temperature. Since all of the simulations in this work were done at a constant temperature, we carried out a series of runs at different temperatures and estimated collision rate constants as a function of temperature as shown in Figure 1. It can be seen that the collision rate constants normalized by the square of the collision radius vary linearly with the square root of the dimensionless temperature.

Note that we do not explicitly specify a solvent density in BD. Instead, we use as input a diffusion coefficient. In order to facilitate comparisons, however, we quote as the "effective solvent density" the density *in the MD simulation which provided the value for the diffusion coefficient.*

Molecular dynamics simulations

We also carried out NVE molecular dynamics simulations of the reaction mixture. A description of this technique is

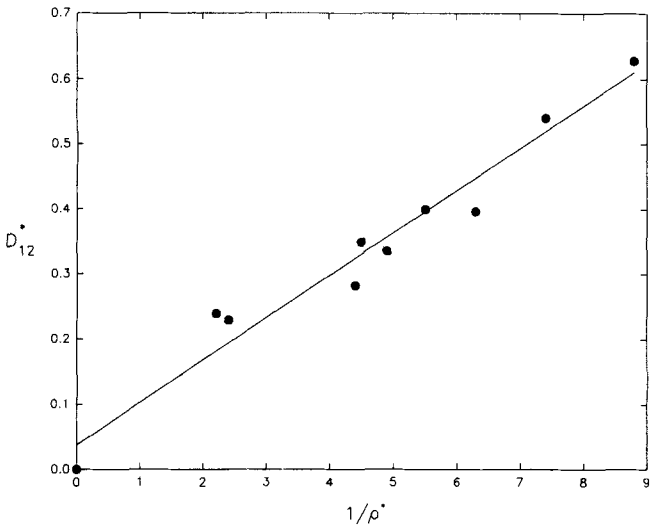

Figure 2. Diffusion coefficient D^*_{12} vs. reciprocal dimensionless density in solvent L-J units, $1/\rho^*$, from very long MD runs.

These diffusion coefficients are computed from time integrals of the velocity autocorrelation function and serve as an input to the BD simulations.

available in the literature (Allen and Tildesley, 1987) and our specific modifications are described in O'Brien et al. (1993). A system of 490 solvent and 10 solute molecules was simulated over various densities. A reduced timestep of $\Delta t^* = 0.003$ (in solvent L-J units) was used. The first 2,000 steps of each run were allowed for equilibration time, after which data collection commenced.

As described above, one of the inputs to the BD simulation is the solute diffusion coefficient D_{12}. In order to provide this diffusivity for a range of densities, a series of very long MD runs of 450,000 steps with a reduced timestep of $\Delta t^* = 0.003$ (corresponding to a total simulated time of about 3 ns) were carried out to measure both the self-diffusivity D_{11} and the cross-diffusivity D_{12} for a series of densities, as shown in Figure 2. The diffusion coefficients were measured by two different techniques using the time-integral of the velocity autocorrelation function and the mean-squared displacements of the solute molecules. The diffusion coefficients computed from each technique were in good agreement with each other.

Kinetics vs. transport: theory

In order to facilitate comparison of our simulation results with the known high-density and low-density behavior of reactions, we review that behavior below. We consider the case of *unactivated* reactions, where all collisions result in reaction (infinitely fast kinetics). For a bimolecular reaction of the form:

$$X + X \xrightarrow{k_{d,x}} Y + Y \tag{3}$$

We can write the reaction rate as:

$$-\frac{d[X]}{dt} = k_{d,x}[X]^2 \tag{4}$$

where $k_{d,x}$ is the reaction rate constant. We can also write the rate of collisions as:

$$\text{collision rate} \equiv \dot{n} = \frac{1}{2} k_{d,c}[X]^2 \tag{5}$$

where $k_{d,c}$ is the collision reaction rate constant, and X is the concentration of the solute molecules which is given by the number of solute molecules per unit volume. We have applied the factor of "1/2" since the rate of reaction is twice the rate of collisions.

At liquid-like densities, the Smoluchowski theory (Smoluchowski, 1917) predicts that diffusional transport limits reaction, and the reaction rate constant varies directly as the diffusivity:

$$k^*_{d,x} = 4\pi R^*_c D^*_{12} \tag{6}$$

Since the diffusion coefficient at the densities that we consider is nearly inversely related to the density, the rate constant predicted from the Smoluchowski theory is inversely proportional to the density and directly proportional to the collision radius. The theory assumes that around each of the reactant molecules, a concentration gradient for the other reactants is set up. The resulting flux of reactant molecules is given by Fick's law, with the boundary condition that the concentration of the reactant molecules is zero at a radius R_c, the collision radius, that is, the minimum distance of approach of two molecules required for reaction to occur. With this boundary condition, the steady-state diffusion equation yields a concentration profile of the form:

$$[X] = [X]_\infty \left(1 - \frac{R_c}{r}\right); \quad r \geq R_c \tag{7}$$

For low densities on the other hand, the kinetic theory of gases (Hirschfelder et al., 1954) predicts that the collision rate constant is given by:

$$k^*_{d,c} = 4\pi (R^*_c)^2 \left(\frac{T^*}{\pi}\right)^{0.5} \tag{8}$$

This is simply the rate of encounter between particles moving at the mean relative thermal velocity. At low densities the rate constants for collision and reaction should be equal, since each measures intrinsic kinetics only under these conditions. Thus the gas kinetic limit predicts a reaction rate constant that is independent of density and is proportional to the square of the collision radius.

Kinetics vs. transport: simulation

We describe now how we compute the rates of collision and reaction in our simulations. The following applies equally to BD and MD, except that we carried out only collision rate measurements using MD, due to the extremely high computational costs.

(*a*) *Collision.* During the course of the simulation, when two particles approach within a distance R_c, we record the beginning of a collision. That collision is deemed to have ended

the first time this pair of particles gets further apart than R_c, at which time we add 1 to the total number of collisions N_{coll} to date. After a simulated time, t, we compute the volumetric collision rate from:

$$\dot{n} = \frac{N_{coll}}{L^3 t} \tag{9}$$

We then compute the collision rate constant, $k_{d,c}$, using Eq. 5.

(*b*) *Reaction.* In order to measure the reaction rate constant using BD, we devised the following scheme (Randolph et al., 1994). At the start of the simulation, all the molecules were "tagged." We defined a collision in the same manner as for the nonreacting system. If two "tagged" molecules collided, then at the end of the collision, we "untagged" the two colliding molecules. Note that molecules were "untagged" only if both the colliding molecules were "tagged" before collision. Even when one of the molecules is "untagged," it continues to be physically present in the simulation and its L-J parameters remain unchanged. This ensures that the system continues to be conservative.

Using this scheme, every time a "reaction" takes place (a pair of "tagged" molecules collides), the number of reactant molecules decreases by two. By recording the time at which each successful reaction occurs, we obtain a concentration vs. time history. Then, integrating Eq. 4, that is, using the standard techniques of chemical kinetic analysis, the slope of the plot of $[X_{tagged}]^{-1}$ against time gives the reaction rate constant $k_{d,x}$.

Results

We carried out collision and reaction measurements over different collision radii. Since the cybotactic radius (or collision radius) R_c varies depending on the nature of the reacting species (that is, whether they are ionic, dipolar, and so on), it is useful to have a measure of how the reaction rate varies with this collision radius. All of the simulations, both MD and BD, were carried out at a reduced temperature of $T_r = 1.08$ (a dimensionless temperature, in solvent units, of $T^* = 1.42$).

Nonreactive collisions

Both BD and MD simulations were used to count the number of collisions that took place over the course of a run. In order to test the dependence of the collision rate constant on both density and collision radius, two sets of experiments were designed for each of the simulation techniques.

Collision Rate Constant as a Function of Density. For BD simulations, the first experiment consisted of carrying out collision number measurements at three different collision radii for each density point. The radii chosen were $R_{c1} = 1.0\ \sigma_{22}$, $R_{c2} = 1.57\ \sigma_{22}$ and $R_{c3} = 2.14\ \sigma_{22}$. The first corresponds to the diameter of the DTBN molecule, the second corresponds to the sum of the DTBN diameter and one ethane solvent shell, while the third corresponds to the sum of the DTBN diameter and two solvent shells. Collision numbers were measured for these three radii for all the densities and collision rate constants were estimated for each radius for a given density using Eqs. 5 and 9.

We found that the collision rate constant $k_{d,c}$ was nearly

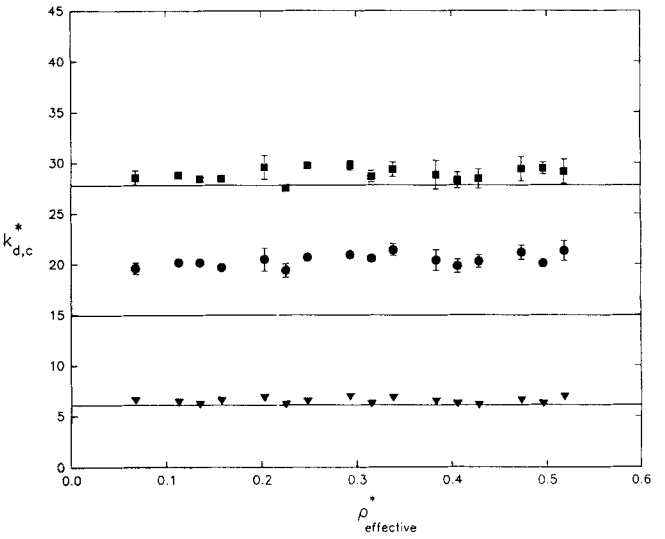

Figure 3. Collision rate constant, $k^*_{d,c}$ vs. effective dimensionless density in solvent L-J units, $\rho^*_{effective}$.

Each of the sets of points corresponds to BD simulations carried out over three different collision radii: ▼, $R_{c1} = 1.0\ \sigma_{22}$; ●, $R_{c2} = 1.57\ \sigma_{22}$; ■, $R_{c3} = 2.14\ \sigma_{22}$; —, results from kinetic theory (nondimensionalized in solute L-J units) for all three collision radii. ⧗, 95% confidence intervals based on 20 measurements. Here $k^*_{d,c}$ is in solute L-J units.

independent of the density of the system for all three collision radii. Also, the value of the collision rate constant corresponded to that predicted from the kinetic theory of gases for the collision radii R_{c1} and R_{c3}, as shown in Figure 3. However, for the collision radius R_{c2}, the two values showed some discrepancy. This difference can be explained from the assumption involved in the derivation of the gas-kinetic limit, which assumes that the number of molecules at any distance r from a given molecule is related to the bulk concentration, whereas it is actually given by the *local* concentration of the fluid at that spatial location. This effect is not seen at R_{c1} and R_{c3}, where the local density nearly matches the bulk density, that is, $g_{22}(R_{c1}) \approx g_{22}(R_{c3}) \approx 1$ (see Figures 6a-6c). At $R_{c2} = 1.57\ \sigma_{22}$, however, this effect would influence the value predicted from kinetic theory.

We carried out the same experiment using MD for the same three collision radii ($R_{c1} = 1.746\ \sigma_{11}$, $R_{c2} = 2.74\ \sigma_{11}$ and $R_{c3} = 3.742\ \sigma_{11}$ in solvent L-J units). The collision rate constants were well predicted from kinetic theory at the smallest collision radius. However, at the higher collision radii, they differed substantially from the kinetic theory result. This is illustrated in Figure 4. The explanation here is the same as that for the collision rate constants from BD. Note that the radial dependence of collision rate constants from MD is solvent-mediated, since solvent affects the radial distribution functions, causing regions of enhancement and depletion to form beyond the first peak. Such effects do not exist in BD simulations where $g_{22}(r)$ is essentially structureless beyond the first peak at all densities.

Collision Rate Constant as a Function of Collision Radius. The second experiment entailed counting collisions over a range of collision radii for a *fixed* density. The same exper-

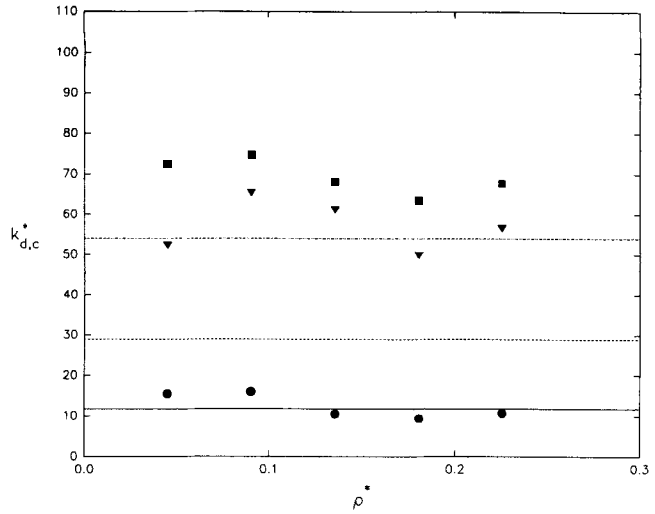

Figure 4. Collision rate constant, $k^*_{d,c}$ vs. dimensionless density in solvent L-J units, ρ^*.

Each of the sets of points corresponds to MD simulations carried out over three different collision radii as follows: ▼, $R_{c1} = 1.746\ \sigma_{11}$; ●, $R_{c2} = 2.74\ \sigma_{11}$; ■, $R_{c3} = 3.742\ \sigma_{11}$. Each line corresponds to the result from kinetic theory for a different collision radius as follows: ——, $R_{c1} = 1.746\ \sigma_{11}$; ----, $R_{c2} = 2.74\ \sigma_{11}$; ·-·-·-·-·-, $R_{c3} = 3.742\ \sigma_{11}$. All of the gas-kinetic limits as well as the rate constant $k^*_{d,c}$ are in solvent L-J units.

iment was carried out using both BD and MD. The rate constant for a given collision radius calculated from these measurements was normalized by the corresponding gas-kinetic limit prediction. This ratio was plotted against the collision radius, as shown in Figures 5a-5c and Figures 6a-6c. The ratio, as a function of radius, appears to be exactly equal to the radial distribution function $g_{22}(r)$. This result makes

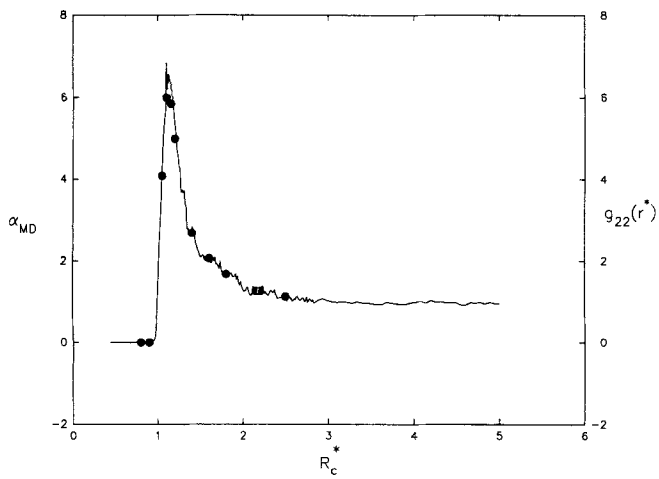

Figure 5a. Effect of collision radius R^*_c (nondimensionalized in solute L-J units) on the collision rate constant, $k^*_{d,c}$: $\rho_r = 0.2909$.

Here α_{MD} is $k^*_{d,c}$ from MD simulations normalized by the gas-kinetic limit. The line is the radial distribution function $g_{22}(r^*)$ obtained from the same MD runs; there is exact quantitative agreement between the two, demonstrating that local density enhancements of solutes around solutes do affect collision rate constants. The density of the system is $\rho_r = 0.2909$.

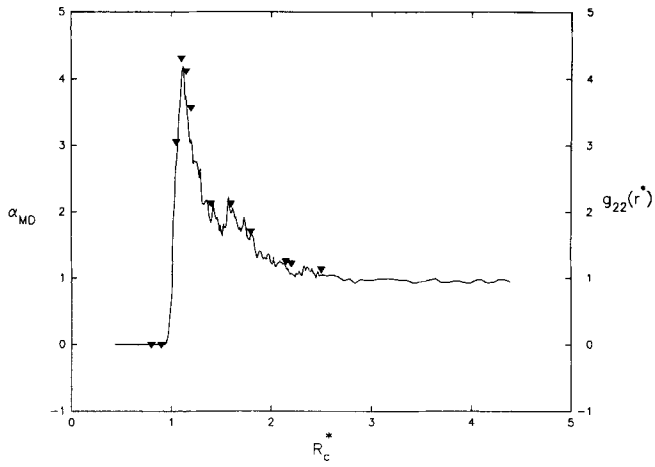

Figure 5b. Effect of collision radius R^*_c on the collision rate constant: $\rho_r = 0.4364$.

Other parameters are the same as in Figure 5a.

sense because the number of solute collisions should be directly related to the local fluid structure surrounding the solute molecules. This is not necessarily the case when a reaction occurs, especially at the higher densities where the equilibrium radial distribution function is eroded by the disappearance of reactant molecules. Rather, the high-density concentration profile obtained under reactive conditions varies as $1/r$.

Reactive collisions

We carried out reaction rate measurements using BD over an effective density range of $\rho_r = 0.1455$ to 1.7455 for the three collision radii that we used for the nonreactive collision dynamics. The plots of $[X_{\text{tagged}}]^{-1}$ vs. time were linear which confirmed the bimolecular nature of this reaction, and these are shown in Figure 7. The reaction rate constant $k_{d,x}$ asymptotically approaches the gas-kinetic limit at low densities and the Smoluchowski limit at high densities for all three collision

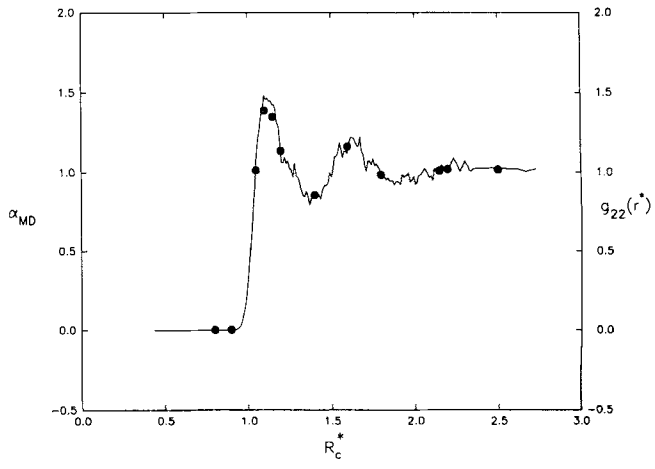

Figure 5c. Effect of collision radius R^*_c on the collision rate constant: $\rho_r = 1.7455$.

Other parameters are the same as in Figure 5a.

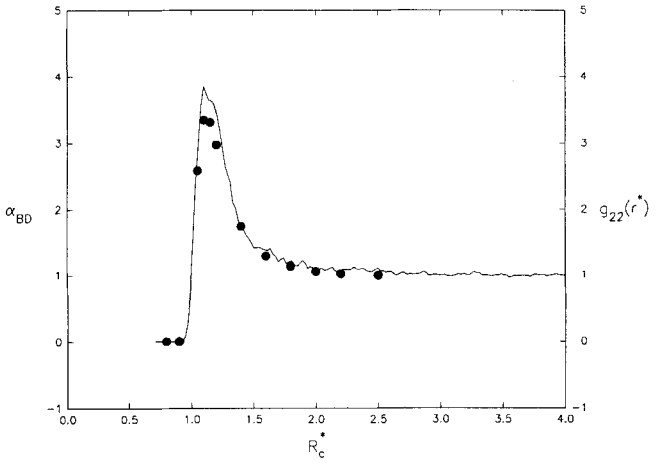

Figure 6a. Effect of collision radius R_c^* (nondimensionalized in solute L-J units) on the collision rate constant, $k_{d,c}^*$: $\rho_{r,\text{eff}} = 0.2909$.

Here α_{BD} is $k_{d,c}^*$ from BD simulations normalized by the gas-kinetic limit. The line is the radial distribution function $g_{22}(r^*)$ obtained from the same BD runs. There is close agreement and this supports the conclusion from MD simulations that solute-solute clustering effects do affect collision rate constants. The effective reduced density of the system is $\rho_{r,\text{eff}} = 0.2909$.

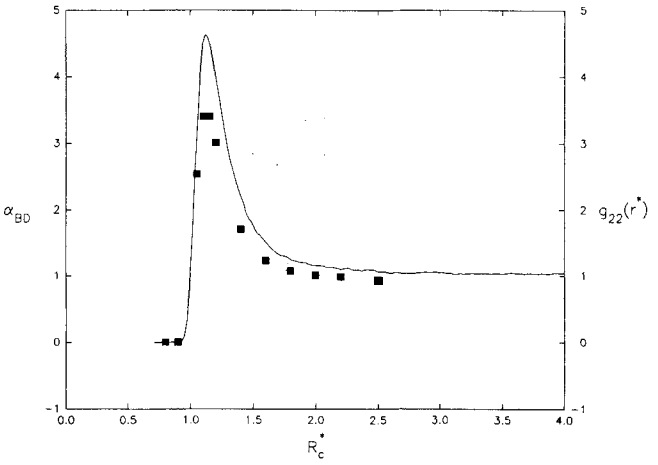

Figure 6c. Effect of collision radius R_c^* on the collision rate constant, $k_{d,c}^*$: $\rho_{r,\text{eff}} = 1.455$.

Other parameters are the same as in Figure 6a.

radii, as shown in Figures 8a–8c. This is consistent with previous reaction studies, which have seen the same transition from collision-limited to diffusion-controlled behavior when moving from the gas to the liquid phase (Otto et al., 1984; Troe, 1986).

To test the dependence of the reaction rate constant on the collision radius, we carried out a series of runs over varying collision radii and density and plotted the reaction rate constant, again normalized by the kinetic theory result, vs. collision radius, as shown in Figures 9a–9c. The radial dependence of this ratio is similar at low densities for both the collision rate constant and the reaction rate constant. This is to be expected since at low densities, the collision rate constant and the reaction rate constant should converge. At higher densities however, the ratio bears a less quantitative resemblance to the equilibrium $g_{22}(r)$ and except at small collision radii begins to drop off as r^{-1}, that is, exactly as the ratio of the Smoluchowski limit to the gas-kinetic limit. In other words, as the reaction changes from being collision-limited at low densities to diffusion-limitation at the higher densities, the radial dependence of this ratio changes from that of the equilibrium $g_{22}(r)$ to a r^{-1} dependence.

Reactive collision simulations using MD would additionally provide information on the effect of solvent-solute clusters on reactivity. However, MD simulations of the same density and concentration ranges as the BD would require simulations having upward of 10^5 molecules in order to obtain adequate statistics. We are currently exploring optimizations (such as parallel computation) that will allow us to carry out these simulations.

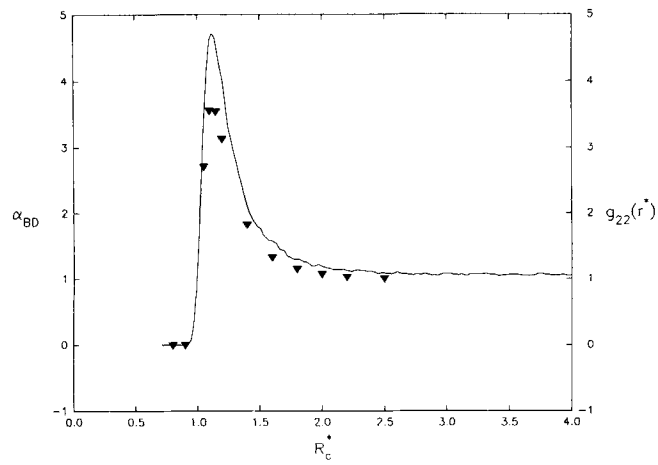

Figure 6b. Effect of collision radius R_c^* on the collision rate constant, $k_{d,c}^*$: $\rho_{r,\text{eff}} = 0.5818$.

Other parameters are the same as in Figure 6a.

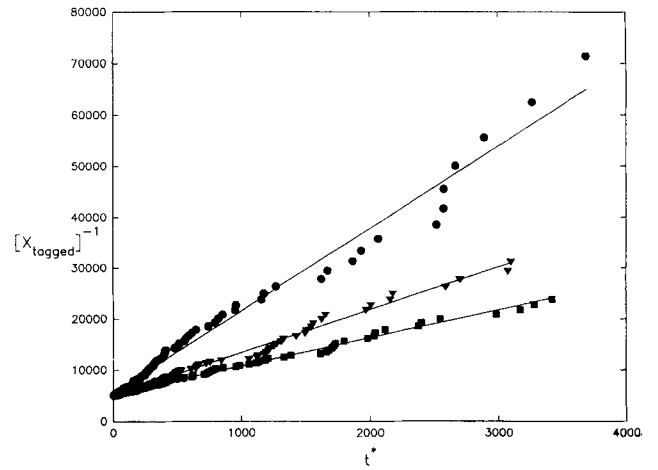

Figure 7. Second-order reaction kinetics plot to determine the reaction rate constant $k_{d,x}^*$ from the reaction BD simulations.

The slope of the line is the rate constant. Each line corresponds to a different effective density as follows: ●, $\rho_{r,\text{eff}} = 0.2909$; ▲, $\rho_{r,\text{eff}} = 0.8727$; ■, $\rho_{r,\text{eff}} = 1.455$. The collision radius is $R_c = 1.57\,\sigma_{22}$.

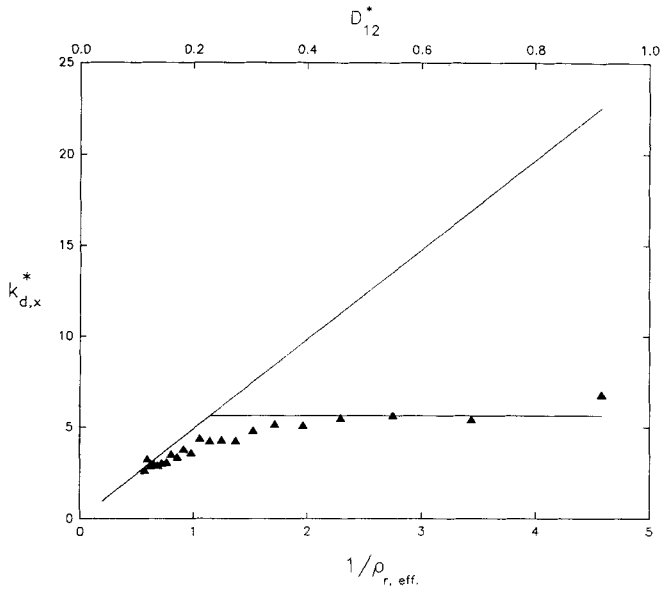

Figure 8a. Reaction rate constant, $k^*_{d,x}$ vs. diffusion coefficient, D^*_{12} in solute L-J units (top axis): $R_c = 1.0\ \sigma_{22}$.

The corresponding effective inverse reduced density, $1/\rho_{r,\text{eff}}$ is also plotted as the lower axis; points are from BD reaction simulations. —— (horizontal) corresponds to the value from kinetic theory, while ------- and —— (skewed) correspond to the Smoluchowski limit. The rate constants from BD asymptotically approach the gas-kinetic line at low densities and the Smoluchowski line at high densities. The collision radius is $R_c = 1.0\ \sigma_{22}$.

Discussion

BD and MD simulations of collision dynamics of solutes in near-critical and supercritical solvents have revealed that collision rate constants are nearly density independent. Also, they are a function of the cybotactic radius and this function is

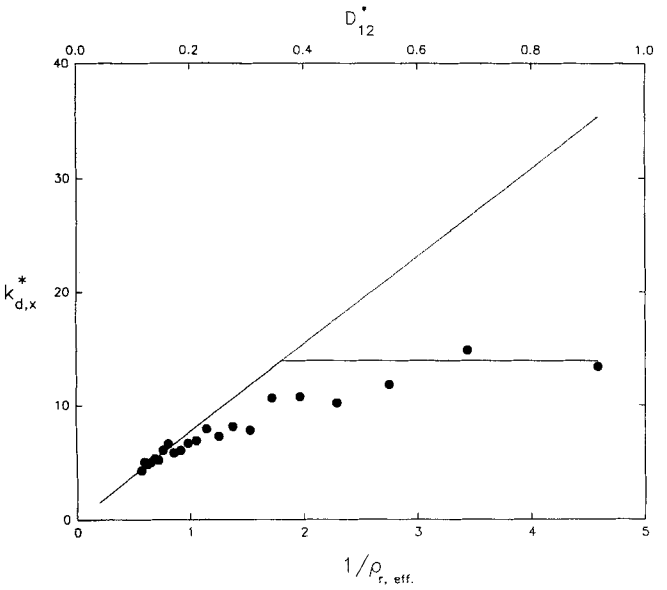

Figure 8b. The effect of collision radius $R_c = 1.57\ \sigma_{22}$ on reaction rate constant.

Other parameters are the same as Figure 8a.

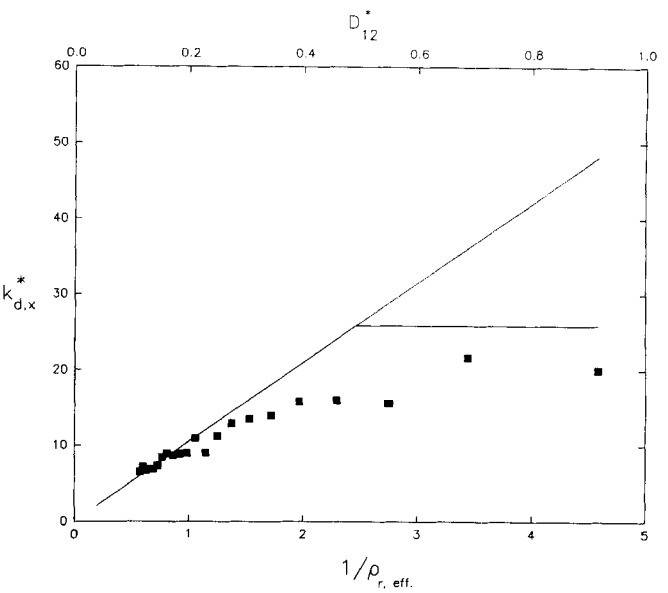

Figure 8c. The effect of collision radius $R_c = 2.14\ \sigma_{22}$ on reaction rate constant.

Other parameters are the same as Figure 8a.

proportional to the solute-solute pair correlation function for all density ranges. Reaction rate constants measured from BD, however, asymptotically approach the gas-kinetic limit at low densities and the Smoluchowski limit at high densities. This is consistent with current understanding of reaction behavior over wide density ranges.

Reaction rate constants appear to reflect solute-solute correlations only at the lower densities. At the higher densities, the reaction becomes diffusion-limited; the consequent concentration gradient around the solute mutes the effect of any equilibrium solute-solute correlation on the reaction rate. It is important to note that the effect of solute-solute correlations on the reaction rate constant also depends on the cybotactic length scale. For a reaction having a cybotactic length scale close to the hard-sphere value, the density range spanning the crossover from dependence on the equilibrium $g_{22}(r)$ to diffusion limitation falls in the near- and supercritical regions.

The density at the crossover from the collision-limited gas-kinetic behavior to the diffusion-limited Smoluchowski behavior increases with decreasing collision radius. The range of densities over which a reaction can be diffusion-limited is therefore a function of the cybotactic radius required for that reaction to occur which, in turn, depends on the nature of the reacting species. For example, the critical exchange distance for Heisenberg spin exchange has been shown to be between one and three times the hard-sphere collision length scale (Bartels et al., 1988). On the other hand, many electron-transfer reactions have a characteristic cybotactic radius of about 10 Å (Goldansky, 1973), corresponding to a dimensionless value of about three hard-sphere diameters. At the same solvent density, two reactions may not be in the same controlling regime, even if each has infinitely fast intrinsic kinetics. Therefore, care must be taken when inferring solvent effects on reactivity on the basis of density alone. This explains some of the apparent inconsistencies when reactions are used as a probe of solvent/solute structure in near- and supercritical fluids.

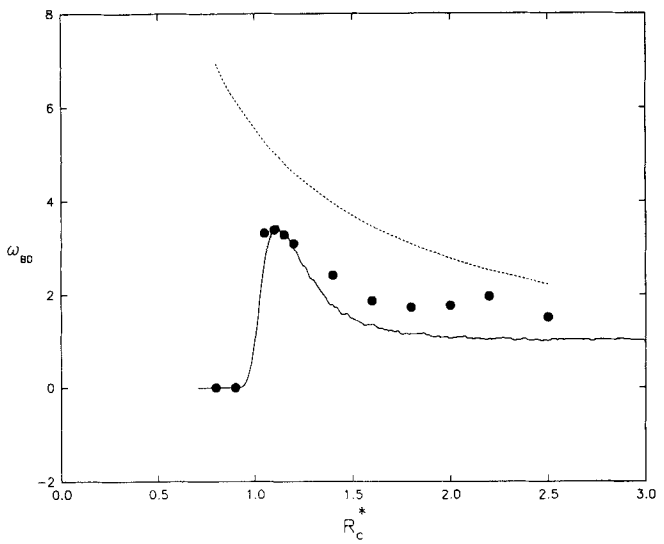

Figure 9a. Effect of collision radius R_c^* (nondimensionalized in solute L-J units) on reaction rate constant, $k_{d,x}^*$: $\rho_{r,\text{eff}} = 0.1455$.

Here ω_{BD} is $k_{d,x}^*$ from BD simulations normalized by the gas-kinetic limit. —— is the equilibrium radial distribution function $g_{22}(r^*)$ obtained from the same BD runs; ------- is the Smoluchowski limit normalized in the same manner. At this density of $\rho_{r,\text{eff}} = 0.1455$, the normalized reaction rate constant data closely resemble the equilibrium $g_{22}(r)$. This indicates that at low densities, when the reaction is collision-limited, the reaction rate constant shows the same radial dependence as the collision rate constant.

Conclusions

BD and MD studies of collision dynamics and BD studies of reaction dynamics have shown that solute-solute clustering affects collision rate constants for all densities, and reaction rate constants only for lower densities. While these studies were carried out for reactions having rapid intrinsic kinetics, local density enhancements of solutes around solutes should affect more strongly reactions that are limited by activation energy constraints; computational studies of such reactions are currently under way. The experimental results appear to support this conclusion: examples of solute-solute clustering affecting reaction rates have been reported for reactions with activation energy limitations (Combes et al., 1992).

The transition between the two limiting regimes for the reaction rate constant depends on both the cybotactic radius for the reaction and the solvent density. Any assumption made regarding the rate-determining step of a reaction should, therefore, be carefully examined. The interplay between these two factors may cause different shifts in the transition region for different reactions; this explains some of the apparent discrepancies that have been reported in the literature.

Finally, we have adapted the Brownian dynamics technique to study reactions in SCFs. Conventionally, BD has been used to investigate equilibrium colloidal (such as Ermak and McCammon, 1978) and nonequilibrium flow (Gupta and Peters, 1985; O'Brien, 1989) problems, but we have suitably modified it to study collision and reaction dynamics with considerable accuracy. When compared with MD techniques which are computationally very intensive, equilibrium BD offers a fast, easily implemented scheme, at the expense of solvent structural information. This technique shows considerable promise as a rapid computational scheme to study microstructure and reactions.

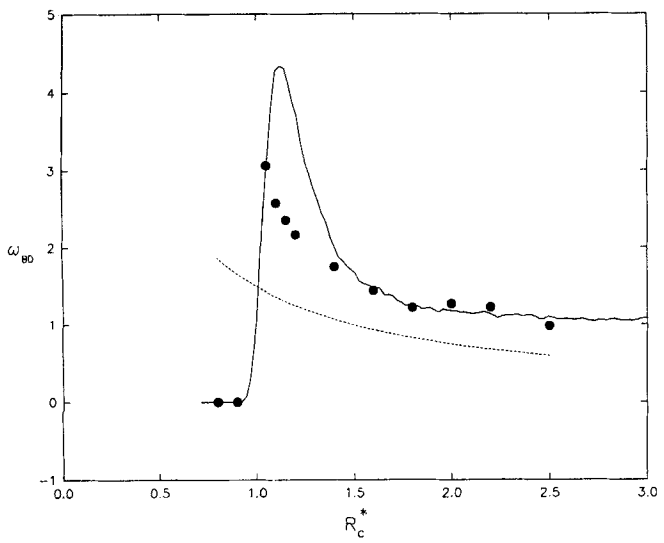

Figure 9b. Effect of collision radius R_c^* on reaction rate constant: $\rho_{r,\text{eff}} = 0.5818$.

For this case, the reaction rate constant data begins to show a dependence that is intermediate between the equilibrium $g_{22}(r)$ and the r^{-1} dependence.

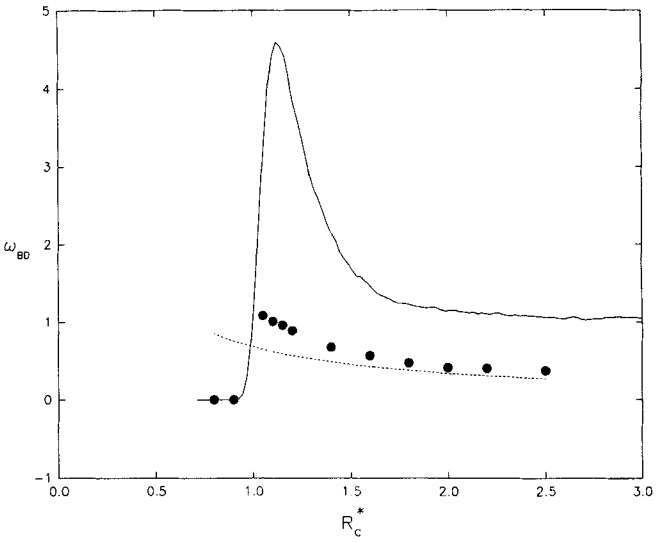

Figure 9c. Effect of collision radius R_c^* on reaction rate constant: $\rho_{r,\text{eff}} = 1.455$.

The data agrees closely with the normalized Smoluchowski limit, which shows that at higher densities, the reaction is indeed diffusion-limited.

Acknowledgments

The authors would like to acknowledge the donors of the Petroleum Research Fund, administered by the American Chemical Society, for partial support of this work (TWR). Further acknowledgment is made to the National Science Foundation for its support through the Pres-

idential Young Investigator Award to TWR and grant CBT-8809548 to JO'B.

Notation

NVE = conditions of constant number of molecules, volume and internal energy (the microcanonical ensemble)
$g(r)$ = radial distribution function
k = Boltzmann constant
L = simulation cube length
m = molecular mass
$\dot{n}$ = volumetric rate of collision
N_{coll} = cumulative number of collisions
r = radial distance, spatial position
r_c = cutoff radius for interactions
R_c = cybotactic or collision radius

Greek letters

α = ratio of the collision rate constant to the gas-kinetic limit
β = Stokesian drag term
$\Gamma(r)$ = Lennard-Jones potential energy function
ϵ = L-J well-depth parameter
ρ = density
σ = L-J length parameter
ω = ratio of the reaction rate constant to the gas-kinetic limit

Subscripts

c = critical property
coll = collision
11 = property of solvent, component 1
12 = solvent-solute cross property
22 = property of solute, component 2
r = reduced property
r,eff = effective reduced parameter

Superscripts

* = dimensionless property/parameter

Literature Cited

Allen, M. P., and D. J. Tildesley, *Computer Simulation of Liquids*, Oxford University Press, New York (1987).

Bartels, D. M., A. D. Trifuac, and R. G. Lawler, "Observations of Heisenberg Spin Exchange Between Reactive Free Radicals," *Chem. Phys. Lett.*, **152**, 109 (1988).

Betts, T. A., J. Zagrobelny, and F. V. Bright, "Elucidation of Solute-Fluid Interactions in Supercritical CF_3H by Steady-State and Time-Resolved Fluorescence Spectroscopy," *Supercritical Fluid Technology, ACS Symp. Ser.*, **448**, 48 (1992).

Brennecke, J. F., and C. A. Eckert, "Fluorescence Spectroscopy Studies of Intermolecular Interactions in Supercritical Fluids," *Supercritical Fluid Science and Technology, ACS Symp. Ser.*, **406**, 14 (1989).

Brennecke, J. F., D. L. Tomasko, and C. A. Eckert, "Naphthalene/Triethylamine Excipilex and Pyrene Excimer Formation in Supercritical Fluid Solutions,"*J. Phys. Chem.*, **94**, 7692 (1990).

Brennecke, J. F., D. L. Tomasko, J. Peshkin, and C. A. Eckert, "Fluorescence Spectroscopy Studies in Dilute Supercritical Solutions," *Ind. Eng. Chem. Res.*, **29**, 1682 (1990).

Brennecke, J. F., and C. A. Eckert, "Molecular Interactions from Fluorescence Spectroscopy," *Proc. Int. Symp. on Supercrit. Fluids*, F. Perrut, ed., Nice, France, p. 263 (1988).

Carlier, C., and T. W. Randolph, "Dense-Gas Solvent-Solute Clusters at Near-Infinite Dilution: EPR Spectroscopic Evidence," *AIChE J.*, **39**(5), 876 (1993).

Chandrasekhar, S., "Stochastic Problems in Physics and Astronomy," *Rev. Mod. Phys.*, **15**, 1 (1943).

Chateauneuf, J. E., C. B. Roberts, and J. F. Brennecke, "Laser Flash Photolysis Studies of Benzophenone in Supercritical Carbon Dioxide," *Supercritical Fluid Technology, ACS Symp. Ser.*, **448**, 48 (1992).

Chialvo, A. A., and P. G. Debenedetti, "On the Use of the Verlet Neighbor List in Molecular Dynamics," *Comput. Phys. Commun.*, **60**, 215 (1990).

Chialvo, A. A., and P. G. Debenedetti, "On the Performance of an Automated Verlet Neighbor List Algorithm for Large Systems on a Vector Processor," *Comput. Phys. Commun.*, **64**, 15 (1991).

Combes, J. R., K. P. Johnston, K. E. O'Shea, and M. A. Fox, "The Influence of Solvent-Solute and Solute-Solute Clustering on Chemical Reactions in Supercritical Fluids," *Supercritical Fluid Technology, ACS Symp. Ser.*, **448**, 31 (1992).

Corti, D. S., and P. G. Debenedetti, "Molecular Dynamics Study of Solute-Solute Interactions in Dilute Supercritical Mixtures," Paper 172b, AIChE Meeting, St. Louis (Nov., 1993).

Debenedetti, P. G., "Clustering in Dilute Binary Supercritical Fluid Mixtures: a Fluctuation Analysis," *Chem. Eng. Sci.*, **42**, 2203 (1987).

Ermak, D. L., and H. Buckholtz, "Numerical Integration of the Langevin Equation: Monte-Carlo Simulation," *J. Comp. Phys.*, **35**, 169 (1980).

Ermak, D. L., and J. A. McCammon, "Brownian Dynamics with Hydrodynamic Interactions," *J. Chem. Phys.*, **69**, 1352 (1978).

Goldansky, V. I., K. I. Zamaraev, A. I. Mikhailov, and R. F. Khairutdinov, "Tunnel Transitions in Electron Transfer Reactions," *Problems of Elementary Reaction Kinetics*, Nauka, Moscow (1973).

Gupta, D., and M. H. Peters, "A Brownian Dynamics Simulation of Aerosol Deposition onto Spherical Collectors," *J. Colloid Interface Sci.*, **104**(2), (1985).

Hirschfelder, J. O., C. F. Curtiss, and R. B. Bird, *Molecular Theory of Gases and Liquids*, Wiley, New York (1954).

Johnston, K. P., S. Kim, and J. Combes, "Spectroscopic Determination of Solvent Strength and Structure in Supercritical Fluid Mixtures: A Review," *Supercritical Fluid Science and Technology, ACS Symp. Ser.*, **406**, 52 (1989).

Johnston, K. P., and C. Haynes, "Extreme Solvent Effects on Reaction Rate Constants at Supercritical Fluid Conditions," *AIChE J.*, **33**, 2017 (1987).

Kajimoto, O., M. Futakami, T. Kobayashi, and K. Yamasaki, "Charge-Transfer-State Formation in Supercritical Fluid: (N,N-Dimethylamino) Benzonitrile in CF_3H," *J. Phys. Chem.*, **92**, 1347 (1988).

Kim, S., and K. P. Johnston, "Molecular Interactions in Dilute Supercritical Fluid Solutions," *Ind. Eng. Chem. Res.*, **26**, 1206 (1987).

Knutson, B. L., D. L. Tomasko, C. A. Eckert, P. G. Debenedetti, and A. A. Chialvo, "Local Density Augmentation in Supercritical Solutions: A Comparison between Fluorescence Spectroscopy and Molecular Dynamics Results," in *Supercritical Fluid Technology, ACS Symp. Ser.*, **448**, 60 (1992).

Kramers, H. A., "Brownian Motion in a Field of Force and the Diffusion Model of Chemical Reactions," *Physica*, **7**, 284 (1940).

McGuigan, D. B., and P. A. Monson, "Analysis of Infinite Dilution Partial Molar Volumes Using a Distribution Function Theory," *Fluid Phase Equilibr.*, **57**, 227 (1990).

North, A. M., *The Collision Theory of Chemical Reactions in Liquids*, Methuen, New York (1964).

O'Brien, J. A., "Brownian Dynamics Simulation of Very Small Particles: Point Source in Uniform Flow," *J. Colloid Interf. Sci.*, **134**, 2 (1990).

O'Brien, J. A., T. W. Randolph, C. Carlier, and S. Ganapathy, "Quasi-critical Behaviour of Dense-Gas Solvent-Solute Clusters at Near-Infinite Dilution," *AIChE J.*, **39**, 1061 (1993).

Otto, B., J. Schroeder, and J. Troe, "Photolytic Cage Effect and Atom Recombination of Iodine in Compressed Gases and Liquids: Experiments and Simple Models," *J. Chem. Phys.*, **81**, 202 (1984).

Prausnitz, J. M., *Molecular Thermodynamics of Fluid Phase Equilibria*, Prentice-Hall, Englewood Cliffs, NJ, p. 107 (1969).

Randolph, T. W., and C. Carlier, "Free Radical Reactions in Supercritical Ethane: A Probe of Supercritical Fluid Structure," *J. Phys. Chem.*, **96**, 5146 (1992).

Randolph, T. W., J. A. O'Brien, and S. Ganapathy, "Does Critical Clustering Affect Reaction Rate Constants? Molecular Dynamics Simulations of Pure Supercritical Fluids," *J. Phys. Chem.*, **98**, 4173 (1994).

Roberts, C. B., Z. Zhang, J. F. Brennecke, and J. E. Chateauneuf, "Laser Flash Photolysis Investigations of Diffusion-Controlled Reactions in Supercritical Fluids," *J. Phys. Chem.*, **97** (1993).

Schroeder, J., and J. Troe, "Elementary Reactions in the Gas-Liquid Transition Range," *Ann. Rev. Phys. Chem.*, **38**, 163 (1987).
Smit, B., P. De Smedt, and D. Frenkel, "Computer Simulations in the Gibbs Ensemble," *Mol. Phys.*, **68**, 931 (1989).
Smoluchowski, M. V. Z., "Versus einer Mathematischen Theorie der Koagulationskinetik Kolloider Lösungen," *Physikal Chem.*, **92**, 129 (1917).
Troe, J., "Elementary Reactions in Compressed Gases and Liquids: From Collisional Energy Transfer to Diffusion Control," *J. Phys. Chem.*, **90**, 357 (1986).
Wu, R.-S., L. L. Lee, and H. D. Cochran, "Structure of Dilute Supercritical Solutions: Clustering of Solvent and Solute Molecules and the Thermodynamic Effects," *Ind. Eng. Chem. Res.*, **29**, 977 (1990).
Yonker, C. R., and R. D. Smith, "Solvatochromism: A Dielectric Continuum Model Applied to Supercritical Fluids," *J. Phys. Chem.*, **92**, 235 (1988).
Zagrobelny, J., and F. V. Bright, "Influence of Solute-Fluid Clustering on the Photophysics of Pyrene Emission in Supercritical C_2H_4 and CF_3H," *J. Am. Chem. Soc.*, **114** (1992).
Zawadzki, A. G., and J. T. Hynes, "Radical Recombination Constants from Gas to Liquid Phase," *J. Phys. Chem.*, **93**, 7031 (1989).

Manuscript received Nov. 29, 1993, and revision received Mar. 21, 1994.